Received: 5 August 2020 | Revised: 15 January 2021 | Accepted: 21 January 2021

DOI: 10.1002/bit.27693

ARTICLE

BIOTECHNOLOGY AND BIOENGINEERING WILEY

Application of metabolic modeling for targeted optimization of high seeding density processes

Matthias Brunner | Klara Kolb | Alena Keitel | Fabian Stiefel | Thomas Wucherpfennig | Jan Bechmann | Andreas Unsoeld | Jochen Schaub

Bioprocess Development Biologicals, Boehringer Ingelheim Pharma GmbH & Co. KG, Biberach, Germany

Correspondence
Matthias Brunner, Bioprocess Development Biologicals, Boehringer Ingelheim Pharma GmbH & Co. KG, Birkendorferstrasse 65, 88397, Biberach, Germany.
Email: matthias.brunner@boehringer-ingelheim.com

Abstract

Process intensification by application of perfusion mode in pre-stage bioreactors and subsequent inoculation of cell cultures at high seeding densities (HSD) has the potential to meet the increasing requirements of future manufacturing demands. However, process development is currently restrained by a limited understanding of the cell's requirements under these process conditions. The goal of this study was to use extended metabolite analysis and metabolic modeling for targeted optimization of HSD cultivations. The metabolite analysis of HSD N-stage cultures revealed accumulation of inhibiting metabolites early in the process and flux balance analysis led to the assumption that reactive oxygen species (ROS) were contributing to the fast decrease in cell viability. Based on the metabolic analysis an optimized feeding strategy with lactate and cysteine supplementation was applied, resulting in an increase in antibody titer of up to 47%. Flux balance analysis was further used to elucidate the surprisingly strong synergistic effect of lactate and cysteine, indicating that increased lactate uptake led to reduced ROS formation under these conditions whilst additional cysteine actively reduced ROS via the glutathione pathway. The presented results finally demonstrate the benefit of modeling approaches for process intensification as well as the potential of HSD cultivations for biopharmaceutical manufacturing.

KEYWORDS
cell culture, high seeding density, N-1 perfusion, process intensification

1 | INTRODUCTION

Increases in biopharmaceutical product approvals over the last years, as well as a high number of molecules currently in clinical development and an anticipated growth of the biosimilar market, will challenge future manufacturing capacities (Bielser et al., 2018; Walsh, 2018). In comparison to today's standard (STD) fed-batch processes, continuous manufacturing has the potential to tremendously enhance the volumetric productivity output (Bielser et al., 2018; Karst et al., 2017; Walther et al., 2019; Xu et al., 2017). Along the way to fully integrated continuous processes, perfusion technology can be used to intensify current fed-batch processes in the already available facilities. Application of perfusion in the N-1 pre-stage bioreactor and a subsequent high seeding density (HSD) in the N-stage process

Abbreviations: CHO, Chinese hamster ovary; HSD, high seeding density; SCD, seeding cell density; TFF, tangential flow filtration; VCD, viable cell density.

has been shown to improve space–time yields in comparison to regular fed-batch processes (Padawer et al., 2013; Pohlscheidt et al., 2013; Xu et al., 2017; Yang et al., 2014).

The objective of this study was to apply extended metabolite analysis and metabolic modeling for targeted optimization of HSD fed-batch cultivations. Although HSD processes have been generally described in literature before, information about the cell metabolism under HSD conditions is still limited. To our knowledge so far only Stepper et al. (2020) investigated HSD cultures in more detail using transcriptome profiling to gather further insights into gene regulations. In this study, a detailed metabolic analysis of an HSD process in comparison to a STD fed-batch process including flux balance analysis (FBA) was performed. This approach revealed distinct metabolic phases with high cell-specific productivities and high formation of reactive oxygen species (ROS) in the HSD process. Based on this analysis an optimized feeding strategy was applied in the HSD processes leading to increased cell-specific productivities, higher cell viabilities, and finally to a strong increase in product titer up to 47%.

2 | MATERIALS AND METHODS

2.1 | Cell lines, seed train, and cultivation processes

Two proprietary CHO-K1 GS cell lines (Cell line A and B) producing a monoclonal antibody (mAb A and B) were cultivated in chemically defined media. Seed train cultures were processed in shake flasks until the N-2 stage. N-1 perfusion cultivations were conducted in 2 L Single-Use Bioreactor (SUB) systems (UniVessel®, Sartorius Stedim Biotech) with the perfusion system KrosFlo® KML™50 (Repligen). Single-use customized Flow Paths (ProConnex®, Repligen) consisting of a modified polyethersulfone (mPES) Tangential Flow Filtration (TFF) membrane (MiniKros®, Repligen) with a pore size of 0.65 µm were used. Recirculation was realized by a centrifugal pump which is included in the KML™50 unit. Recirculation flow and perfusion rate were controlled by the KML™50 system according to the specific setpoints. N-1 perfusion cultures for the inoculation of the HSD and STD fed-batch processes were processed for 6 days and the perfusion rate was adjusted every 24 h by the reactor volumes per day. HSD and STD fed-batch cultivations were inoculated from N-1 perfusion cultures with 10×10^6 cells/ml (HSD) or 0.7×10^6 cells/ml (STD), respectively and conducted for up to 14 days in 3 L glass bioreactor systems (Applikon Biotechnology). pO_2, temperature, pH, and P/V settings were identical in the HSD and STD fed-batch process. Feed medium was added continuously from Day 0 (HSD) or Day 1 (STD) until the end of the process. Glucose was added to the process on demand. HSD processes indicated as HSD LAC, HSD LAC/CYS, and HSD CYS cultivations included bolus additions of sodium lactate (bolus criteria: ≤2 to 3 g/L) and/or cysteine (fixed bolus: Day 1 to Day 5), respectively.

2.2 | In-process analytics and LC-MS/MS measurements

Cultivation samples were taken every 24 h and cell counting and viability determination was performed using a Cedex HiRes analyzer (Roche). The metabolites glucose, lactate, and ammonia were measured with a Konelab™ Prime60i (Thermo Fisher Scientific) device. Antibody concentration was determined with a Protein-A HPLC method (Thermo Fisher Scientific). Amino acid analytics were performed with a 7890B GC system (Agilent Technologies). Cysteine was excluded from the amino acid method due to the known stability issues of this component (Prade et al., 2020; Wang et al., 2017). LC-MS/MS was applied to determine vitamin concentrations and additional metabolites such as 2-hydroxybutyrate, indole-3-lactic acid, indole-3-carboxylic acid, and 2-deoxycitidine. LC-MS/MS samples were measured using an InfinityLab Poroshell Hydrophilic interaction chromatography (HILIC)-Z column (Agilent Technologies) as described previously (Krattenmacher et al., 2018). Tandem mass spectrometry was performed on a QTRAP® 6500 + triple quadrupole mass spectrometer (Sciex) equipped with an ESI source and coupled to an Agilent 1260 series binary HPLC system (Agilent Technologies). Nitrogen was used as curtain and collision gas. Data were acquired using MultiQuant 3.0.3 software (Sciex).

2.3 | Flux balance analysis

FBA was performed with the software Insilico Inspector™ (Insilico Biotechnology). The software uses a genome-based metabolic network model of the used CHO-K1 cell line as described previously in Schaub et al. (2012). The FBA was performed under a metabolic steady state with constant growth and specific rates of metabolites similar to Popp et al. (2016). As an objective function, the maximization of ATP production was used to calculate intracellular fluxes similar to Ivarsson et al. (2015). The glycolytic activity was defined by the flux from fructose-1, 6-biphosphate to glyceraldehyde-3-phosphate and the TCA activity by the formation of citrate from oxaloacetate, under incorporation of acetyl-coA according to Wahrheit et al. (2014). ROS production rates were calculated based on the flux of complex I of the electron transport chain since this is the main source for mitochondrial ROS production (Zhao et al., 2019).

3 | RESULTS AND DISCUSSION

3.1 | Metabolic analysis of HSD processes

The process performance of HSD cultivations, conducted with cell line A, was analyzed and compared to STD fed-batch processes including data of cell growth and product titer as well as several metabolites (Figure 1). HSD cultivations, inoculated at 10×10^6 cells/ml, were

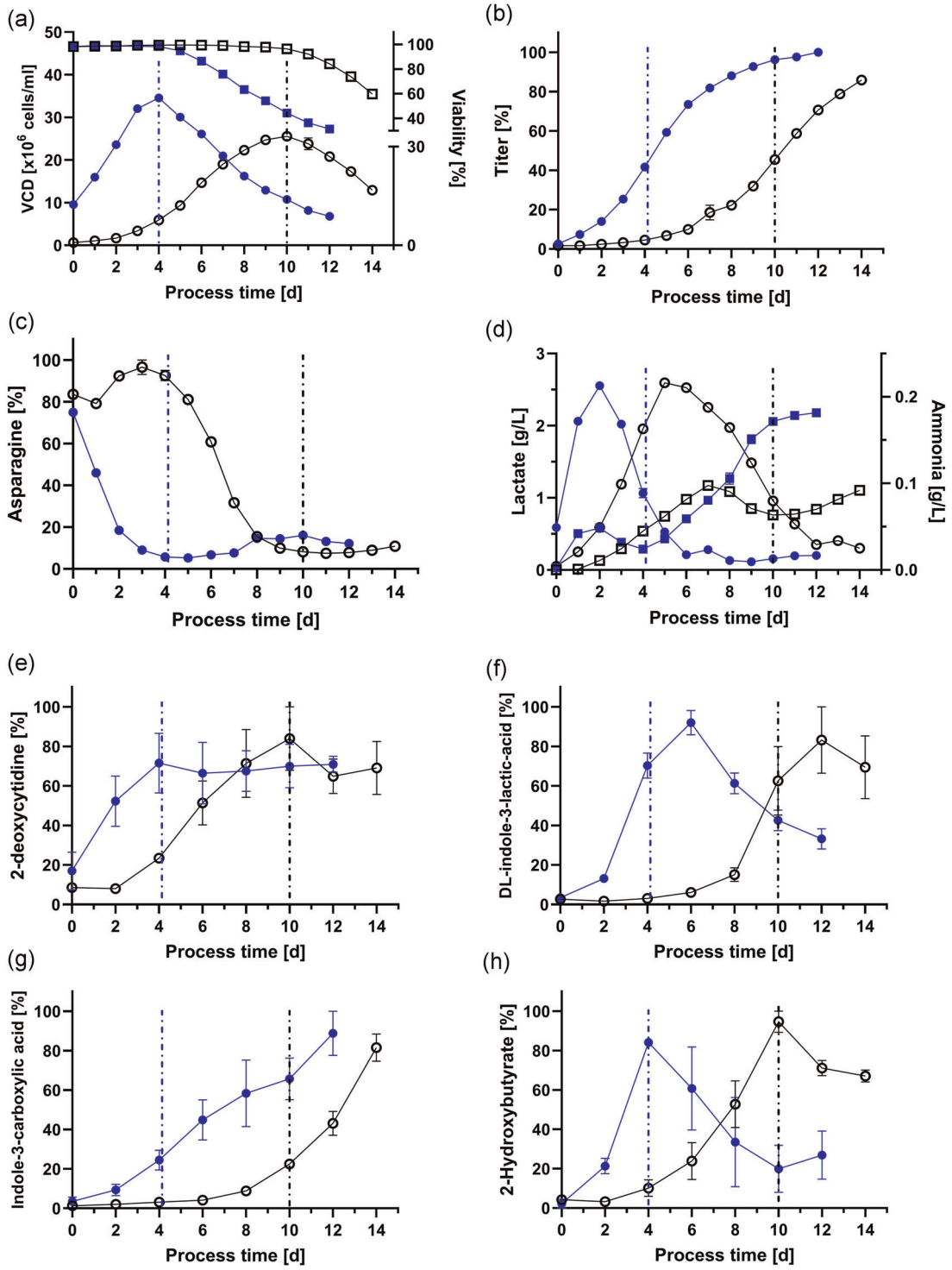

FIGURE 1 (a) VCD (STD; HSD) and viability (STD; HSD), (b) titer (STD; HSD), (c) asparagine (STD; HSD), (d) lactate (STD; HSD) and ammonia (STD; HSD) concentrations, (e) 2-deoxycytidine concentration (STD; HSD), (f) DL-indole-3-lactic-acid concentration (STD; HSD), (g) Indole-3-carboxylic acid concentration (STD; HSD), and (h) 2-hydroxybutyrate concentration (STD; HSD) over process time. All experiments were conducted in duplicates ($n = 2$). Vertical dotted lines indicate the timepoint of the drop in cell viability in HSD and STD cultures. HSD, high seeding densities; STD, standard; VCD, viable cell density [Color figure can be viewed at wileyonlinelibrary.com]

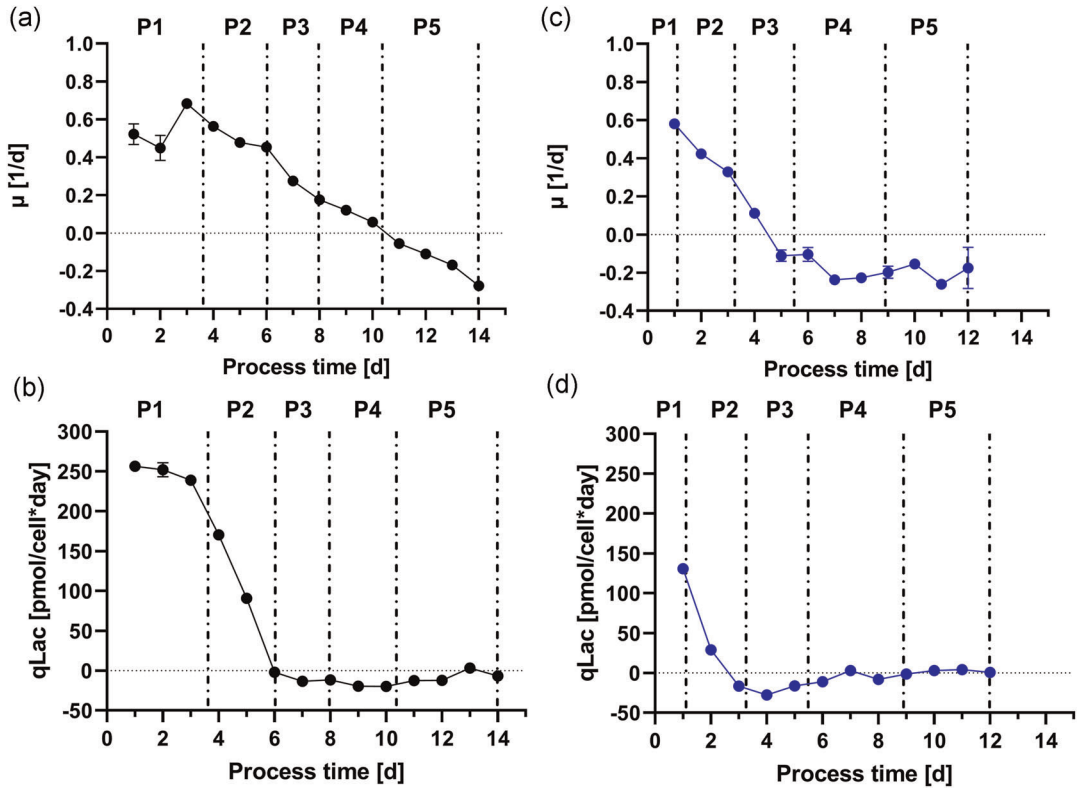

FIGURE 2 Metabolic phases P1 to P5 and corresponding cell-specific growth rate (μ) and specific lactate production (qLac) over process time for the STD cultivations (a and b; $n = 2$) and HSD cultures (c and d; $n = 2$). HSD, high seeding densities; STD, standard [Color figure can be viewed at wileyonlinelibrary.com]

characterized by a higher peak VCD when compared to the STD process and an early viability drop starting at process Day 4, leading to low viabilities under 40% at Day 12 (Figure 1a). Due to the high amount of viable cells in the HSD bioreactor, the product concentration strongly increased early on in the process but the rise in titer declined from Day 6 on, leading to a final enhancement in product titer of 15% compared to the STD conditions (Figure 1b). However, the same titer as in the STD processes was reached already between Day 7 and Day 8 in the HSD cultivations which significantly increased space–time yields. These general findings are in good agreement with other publications of HSD processes as Padawer et al. (2013) and Pohlscheidt et al. (2013). To further characterize and compare the cultivations, several metabolites were investigated including amino acids, vitamins and substances recently reported to be related with growth inhibition or apoptosis (Chong et al., 2011; Mulukutla et al., 2017). No nutrient depletion was observed from the amino acid, vitamin, and glucose analysis, neither in the HSD nor in the STD cultivations. The only nutrient, which reached low concentrations close to the timepoint of the viability drop of the HSD and STD processes, was asparagine (Figure 1c). Asparagine is a non-essential amino acid and uptake in CHO cells is especially high during the growth phase (Ritacco et al., 2018). However, low concentrations or even asparagine exhaustion have been shown in the literature to not be the root cause for onset of stationary growth or even VCD decrease (Duarte et al., 2014; Ghaffari et al., 2019). Another reason for the viability break down could be the accumulation of potentially inhibiting or toxic metabolites. HSD processes did show an early lactate metabolic shift from lactate production to consumption on Day 2 and a higher final ammonia concentration when compared to the STD processes. However, lactate concentrations of both processes reached a maximum of approx. 2.5 g/L and ammonia concentrations during the growth phase stayed below 0.1 g/L. These values are below reported growth inhibiting or toxic concentrations (Hansen & Emborg, 1994; Lao & Toth, 1997; Lindskog, 2018). Besides lactate and ammonia, other potentially growth inhibiting or apoptosis-inducing metabolites have been reported recently (Chong et al., 2011; Mulukutla et al., 2017; Pereira et al., 2018). To further investigate the sudden decrease in VCD in the HSD cultures, several of these metabolites such as 2-deoxycitidine, indole-3-lactic acid, indole-3-carboxylic acid, and 2-hydroxybutyrate were analyzed (Figure 1e-h). Interestingly, all substances did show a similar concentration in the HSD and STD culture at the timepoint when cell viabilities started to decrease. Additionally, three of these metabolites reached their peak concentrations close to the viability drop in both culture types. Deoxycitidine has been shown before by Chong et al. (2011) to be positively correlated with increased caspase activities and cell apoptosis. Mulukutla et al. (2017) did report the inhibiting effects of indole-3-lactic acid, indole-3-carboxylic acid, and 2-hydroxybutyrate on cell growth and that strong synergistic effects of these metabolites have to be considered. The next step to gain further insights into the

cell's metabolism under HSD and STD culture conditions was to use FBA.

FBA was applied under the steady-state assumption, dividing the HSD and STD processes into five metabolic phases (P1–P5) (Figure 2a–d). Notably, cell metabolism of STD and HSD processes were already different in metabolic phase 1. STD cultures were characterized by a prolonged exponential growth phase with constant specific cell growth (Figure 2a) and high uptake and release rates of glucose and lactate (Figures 2b and 3a). The HSD processes displayed a similar initial cell growth but had a significantly shorter phase 1 and strongly reduced specific glucose uptake and lactate production. Additionally, HSD processes in phase 1 revealed an increased alanine and glycine release, reduced tyrosine uptake, and an increased asparagine uptake rate (Figure 3a). Metabolic phases 2 and 3 were characterized by the switch from lactate production to consumption in both cultivation types. In contrast to the STD cultivations, lactate consumption in the HSD processes started already in phase 2 and specific cell growth became negative in phase 3 whereas in the STD processes only the last metabolic phase (P5) showed negative growth rates. Metabolic phases 4 and 5 in the HSD processes were characterized by almost constant negative specific growth rates and very low glucose uptake and lactate release rates. It is surprising that cell growth did already decrease in the HSD cultivations after Day 1 since both STD and HSD cultivations were inoculated from the same N-1 perfusion stage. However, it could be explained by the fast accumulation of growth-inhibiting substances caused by the high cell densities present in the culture (Figure 1d–h). Different split ratios and therefore different ratios of consumed medium carryover and fresh medium at inoculation could have been another factor contributing to a different cell environment at process start. However, only minor differences for glucose (20%), serine (11%), and asparagine (11%) starting concentrations (data not shown) and almost no differences in several potential inhibitory substances such as ammonia, 2-hydroxybutyrate, indole-3-carboxylic acid, and indole- 3-lactic acid (Figure 1d–h) were observed. The highest difference was the initial lactate concentration with below limit of detection < 0.1 g/L (STD) compared to 0.5 g/L (HSD).

Through application of the FBA, it was possible to generate data of the intracellular metabolism. Figure 3b shows the intracellular fluxes of glycolysis, TCA cycle, and pentose phosphate pathway (PPP) as well as the ratio of TCA/glycolytic activity for all five metabolic phases of the STD and HSD cultivations. A more detailed

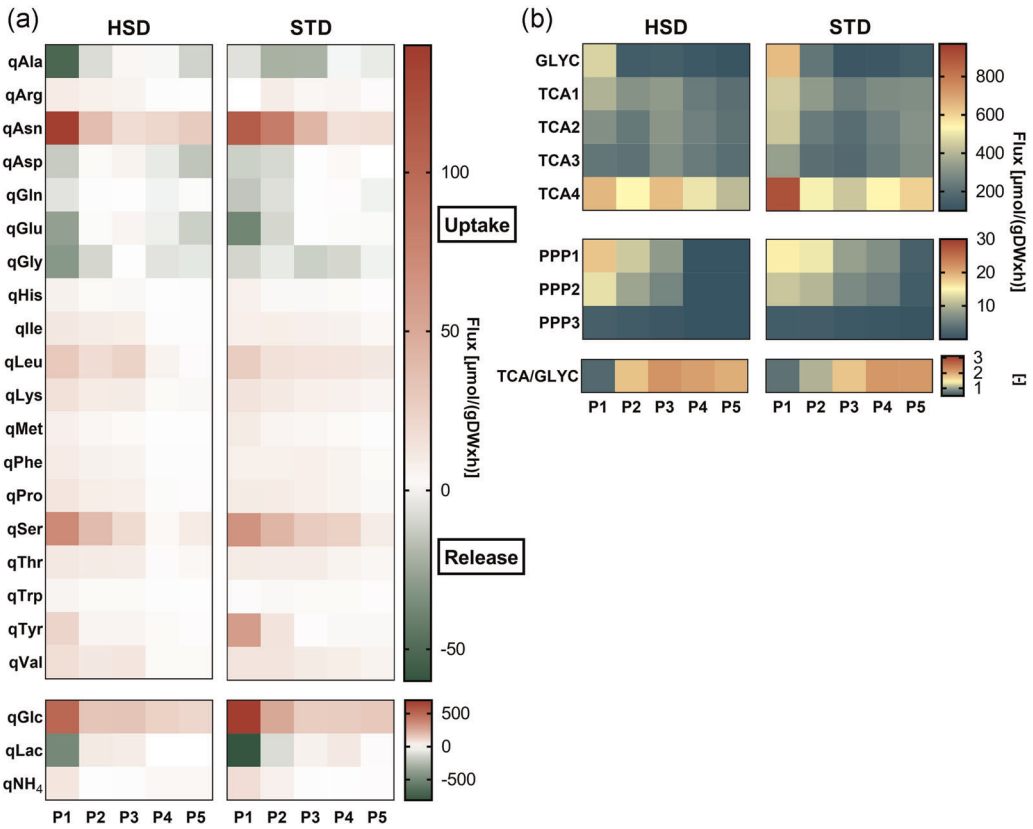

FIGURE 3 (a) Heat map of the specific amino acid, glucose, lactate, and ammonia uptake and release rates for the metabolic phases of the STD ($n = 2$) and HSD ($n = 2$) processes. (b) Heat map of intracellular fluxes of glycolysis (GLYC), TCA cycle (TCA1-4), pentose phosphate pathway (PPP1–3), and the ratio of TCA to glycolytic activity (TCA/GLYC) for the metabolic phases of the STD ($n = 2$) and HSD ($n = 2$) processes. GLYC, F1,6BP to GAP; TCA1, Pyr to AcCoA; TCA2, Cit to AKG; TCA3, AKG to Suc; TCA4, Mal to OAA; PPP1, G6P to 6P-gluconate; PPP2, R5P to nucleotide synthesis; PPP3, sum of fluxes from ribulose-5P and xylulose-5P to F6P and GAP. The values of all calculated fluxes and rates are reported in Table S1. GLYC, glycolysis; HSD, high seeding densities; PPP, pentose phosphate pathway; STD, standard; TCA, tricarboxylic acid [Color figure can be viewed at wileyonlinelibrary.com]

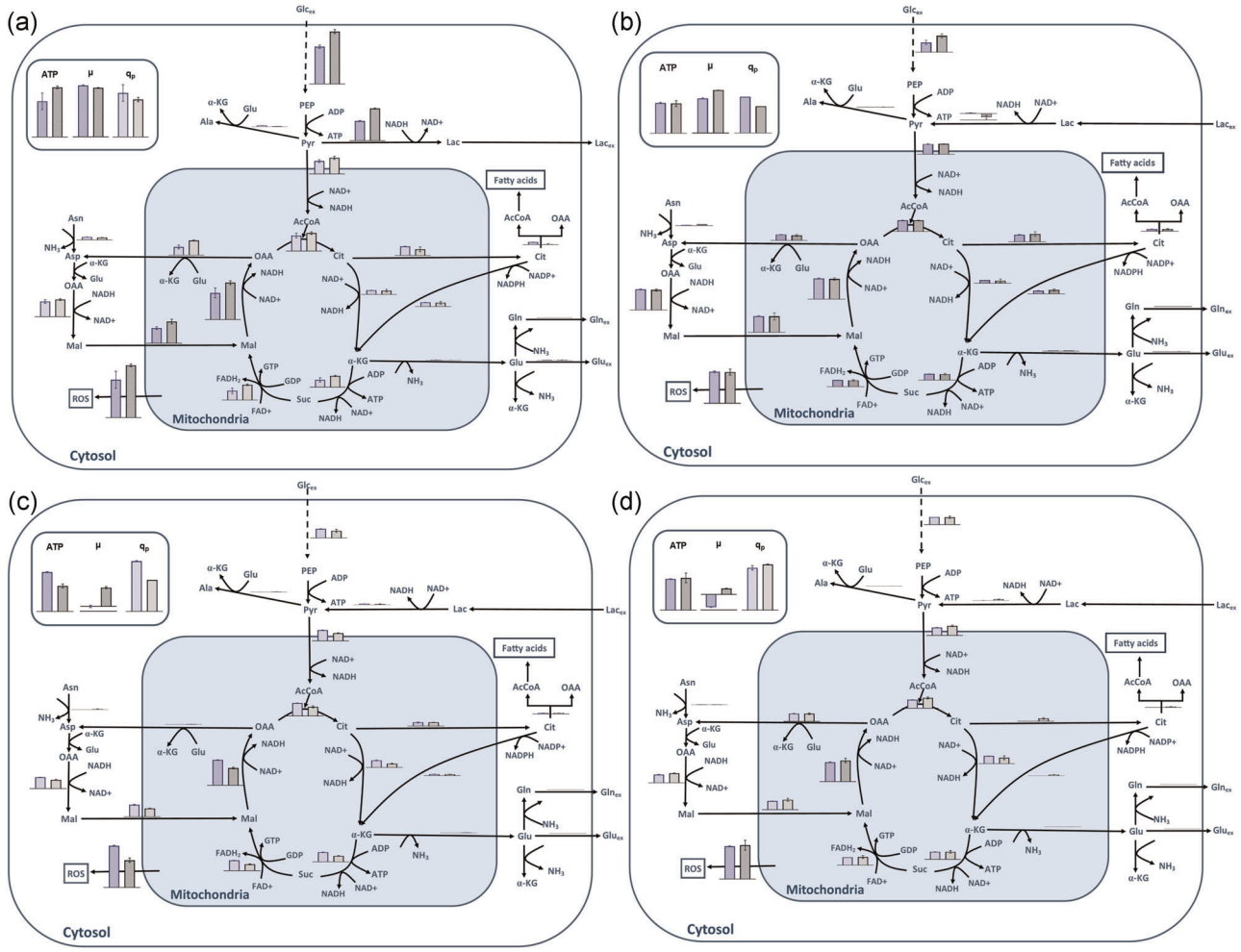

FIGURE 4 Intracellular fluxes, ATP and ROS formation as well as specific cell growth (μ) and specific productivity (q_p) of the metabolic phases 1 to 4 (a–d) of the HSD (blue; $n = 2$) and STD (gray; $n = 2$) processes. All fluxes are normalized to the highest flux over all metabolic phases and cultivations. The values of all calculated fluxes and rates are reported in Table S2. HSD, high seeding densities; ROS, reactive oxygen species; STD, standard [Color figure can be viewed at wileyonlinelibrary.com]

presentation of the most prominent intracellular fluxes of glycolysis and TCA cycle as well as corresponding ATP, ROS formation, and specific product formation rates is given in Figure 4a–d. Fluxes of the PPP were very low in all phases (around 5% of the glycolytic influx) for both process types (Figure 3b). This is similar to reported data from Schaub et al. (2012) and Becker et al. (2019) but in contrast to Sengupta et al. (2011) and Ahn and Antoniewicz (2011) who reported high fluxes into the PPP in the non-exponential phase. However, strong variations between 9% and 43% of PPP flux between different cell lines were reported from Goudar et al. (2010) with hybridoma cell lines. Cell line-specific effects might therefore explain the very low PPP fluxes in this study. The shift from lactate production to consumption in phase 2 of the HSD cultivations was associated with a reduced glucose consumption resulting in a higher ratio of TCA to glycolytic activity when compared to the STD processes (Figure 3b). Although TCA fluxes and total ATP production in this phase were similar, the HSD cultivations displayed a reduced specific cell growth and increased specific productivity (Figure 4b). Phase 3 of the HSD cultivations was characterized by the highest rates of ATP production, cell-specific productivity, formation of ROS, and a high specific lactate uptake (Figures 4c and 2d). At the same time a strong drop in specific cell growth to negative values could be observed in this phase, which could be related to the increased production of intracellular ROS species. High ROS levels are known to have detrimental effects on cells, affecting proteins, lipids, RNA, and DNA (Chevallier et al., 2020; Forkink et al., 2010) and potentially leading to cell death via apoptosis (Henry et al., 2020). In phase 4, HSD and STD processes showed similar ATP production, specific productivities, glycolytic and TCA cycle fluxes but a strongly opposed growth behavior (Figure 4d). Although cells in phase 5 of the STD cultivations are dominated by negative cell growth values, the metabolic activity was higher than in the HSD processes (Figure 3b).

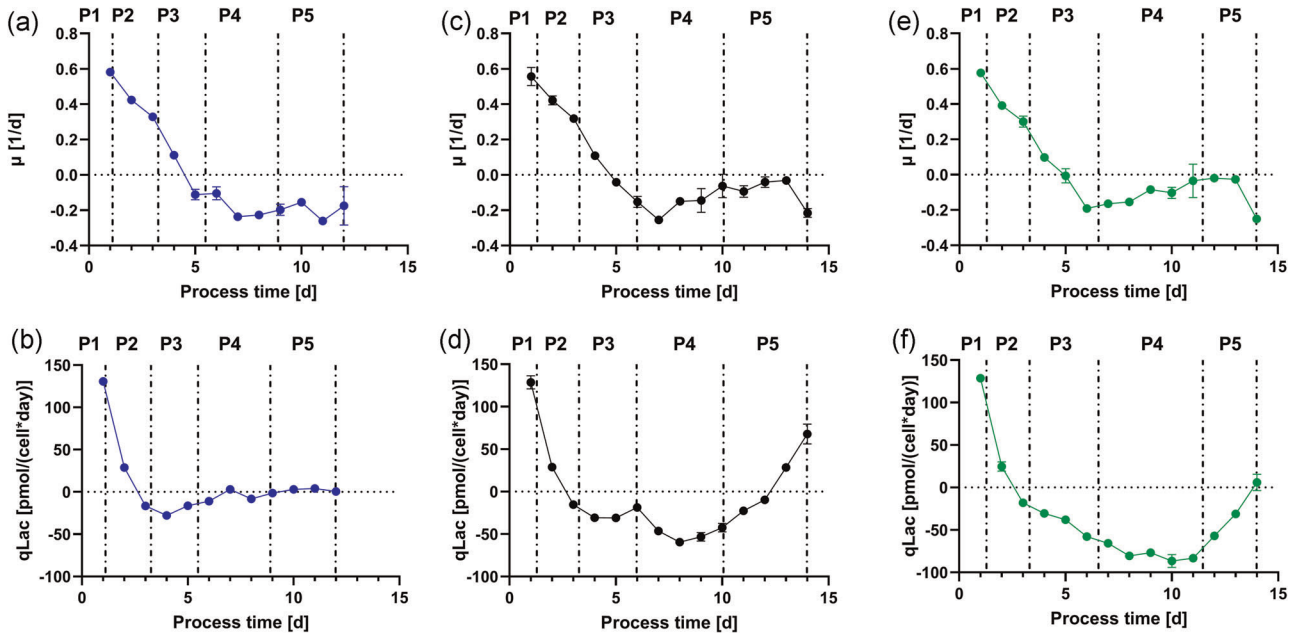

FIGURE 5 Metabolic phases P1 to P5 and corresponding cell-specific growth rate (μ) and specific lactate production (qLac) over process time for the HSD cultivations (a and b; $n = 2$) and HSD cultures supplemented with lactate (HSD LAC) (c and d; $n = 2$) and HSD cultures supplemented with lactate and cysteine (HSD LAC/CYS) (e and f; $n = 2$). CYS, cysteine; HSD, high seeding densities; LAC, lactate [Color figure can be viewed at wileyonlinelibrary.com]

3.2 | Optimization of HSD cultivations

After the metabolic characterization of the HSD cultivations, the goal was to further optimize the processes with respect to their volumetric productivity, explicitly targeting cell viabilities and cell-specific productivities. Based on the fact that the highest specific productivities were achieved in metabolic phase 3 (Figure 4c) and previously generated in-house data, published from Stepper et al. (2020), we hypothesized that additional supplementation of the cultures with lactate might be beneficial to increase cell-specific productivities. Furthermore, we speculated that the high formation of ROS in the metabolic phase 3 did lead to increased apoptosis and thus to the strong decrease in viable cell density. Cysteine supplementation has been shown before in literature to improve cell viabilities in HSD processes by an increase of the intracellular glutathione concentration and thereby actively reducing ROS (Ali et al., 2018). Additional HSD processes were conducted with further supplementation of lactate in combination with cysteine. Subsequently, FBA was performed on processes supplemented only with lactate (HSD LAC) and processes with a combination of lactate and cysteine supplementation (HSD LAC/CYS).

In comparison to the HSD cultivations, the lactate and lactate/cysteine supplemented cultures did show a similar metabolism in metabolic phase 1 and phase 2 with comparable growth rates as well as specific uptake and production rates of glucose, lactate, and amino acids (Figures 5 and 6a). In contrast, phases 3 and 4 displayed strong metabolic differences with increased specific lactate uptake and a prolonged metabolic phase 4 with even more pronounced effects in the HSD LAC/CYS culture than in the HSD LAC cultivation. Specific growth rates in phases 4 and 5 did deviate strongly from the HSD process in the LAC and LAC/CYS supplemented cultures. Amino acid profiles were similar between HSD, HSD LAC, and HSD LAC/CYS cultures during all metabolic phases, with only slight differences in the alanine, aspartate and glutamate metabolism (Figure 6a). The increased uptake of lactate in the supplemented cultures did correlate with a decrease in glucose consumption (Figure 6c). This is in accordance with Mulukutla et al. (2012) who reported reduced glycolytic fluxes associated with lactate consumption and increased extracellular lactate concentrations. This observation further resulted in a higher activity of the TCA cycle in comparison to the glycolytic pathway for the HSD LAC and HSD LAC/CYS cultures (Figure 6b).

A more detailed picture of the cells metabolism in metabolic phases 3 and 4 under HSD control and HSD LAC/CYS supplemented conditions is presented in Figure 7. Although cysteine was not measured, due to its known stability issues (Prade et al., 2020; Wang et al., 2017) and therefore not included in the FBA, the reaction pathways of cysteine are presented in Figure 7. Whereas lactate uptake and glucose consumption in metabolic phase 3 differed between the processes, the TCA cycle fluxes and thus ATP and ROS level were comparable (Figure 7a). However, specific productivities were slightly increased and specific cell growth slightly decreased under LAC/CYS supplemented conditions. In metabolic phase 4, the increased consumption of lactate in HSD LAC/CYS cultivations did correlate with a strong reduction of the glucose consumption, resulting in an overall lower flux from pyruvate into the TCA cycle (Figure 7b). This reduction in the TCA cycle flux did finally lead to a lower ATP and ROS production. At the same time, specific cell

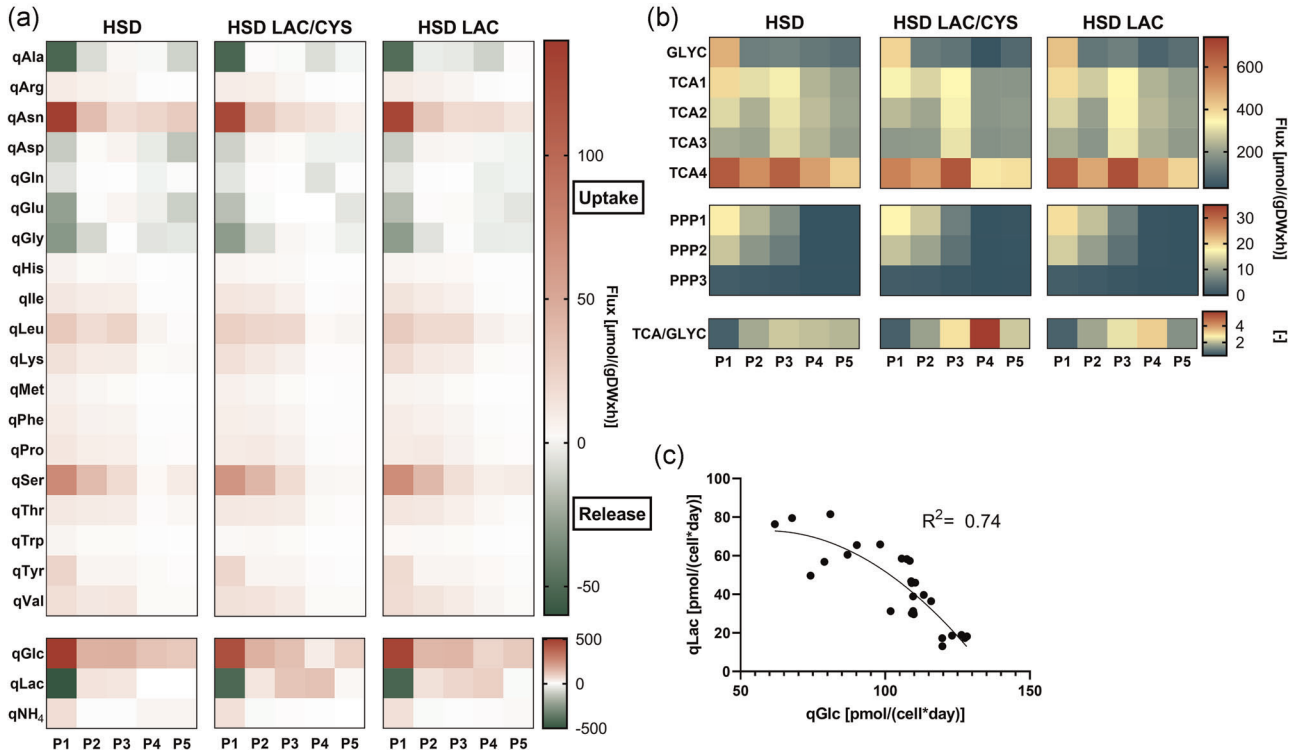

FIGURE 6 (a) Heat map of the specific amino acid, glucose, lactate, and ammonia uptake and release rates for the metabolic phases of the HSD cultures ($n = 2$) and HSD cultures supplemented with lactate (HSD LAC; $n = 2$) and HSD cultures supplemented with lactate and cysteine (HSD LAC/CYS; $n = 2$). (b) Heat map of the intracellular fluxes of glycolysis, TCA cycle, pentose phosphate pathway, and the ratio of TCA to glycolytic activity for the metabolic phases of the HSD ($n = 2$) and HSD cultures supplemented with lactate (HSD LAC; $n = 2$) and HSD cultures supplemented with lactate and cysteine (HSD LAC/CYS; $n = 2$). (c) Correlation of the specific lactate uptake (qLac) with specific glucose uptake rate (qGlc) of the HSD LAC and HSD LAC/CYS cultivations. The values of all calculated fluxes and rates are reported in Table S3. CYS, cysteine; GLYC, glycolysis; HSD, high seeding densities; LAC, lactate; PPP, pentose phosphate pathway; TCA, tricarboxylic acid [Color figure can be viewed at wileyonlinelibrary.com]

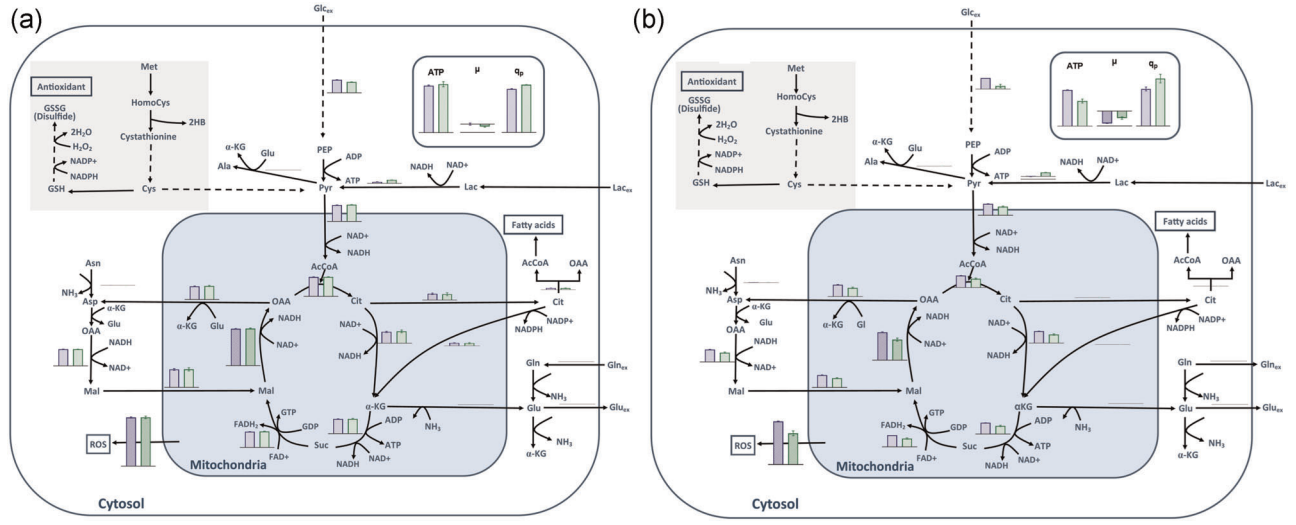

FIGURE 7 Intracellular fluxes, ATP and ROS formation as well as specific cell growth (μ) and specific productivity (q_p) of the metabolic phases 3 (a) and 4 (b) of the HSD (blue; $n = 2$) and HSD LAC/CYS (green; $n = 2$) processes. All fluxes are normalized to the highest flux over all metabolic phases and cultivations. Cysteine metabolism is shaded in gray as cysteine measurements were not included in the FBA. The values of all calculated fluxes and rates are reported in Table S4. CYS, cysteine; HSD, high seeding densities; LAC, lactate; ROS, reactive oxygen species [Color figure can be viewed at wileyonlinelibrary.com]

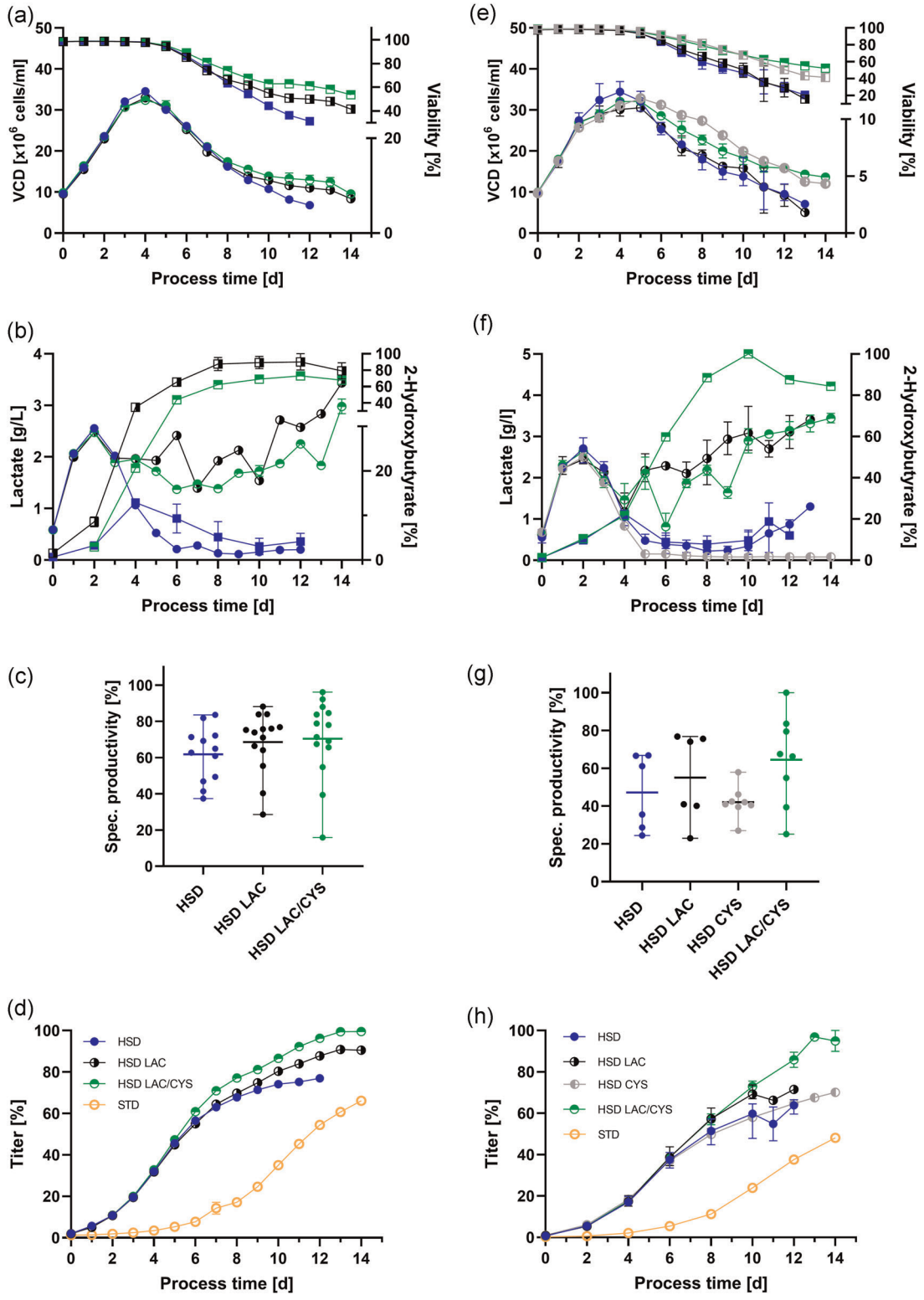

FIGURE 8 Process performance of the optimized HSD cultures for (a–d) cell line A and (e–h) cell line B. (a) VCD (HSD; HSD LAC; HSD LAC/CYS) and viability (HSD; HSD LAC; HSD LAC/CYS) and (b) lactate (HSD; HSD LAC; HSD LAC/CYS) and 2-hydroxybutyrate (HSD; HSD LAC; HSD LAC/CYS) over process time. (c) Specific productivity of HSD, HSD, and HSD LAC/CYS cultivations during the entire process with mean and range. (d) Product titer over culture duration of the HSD cultivations compared to the STD fed-batch. (e) VCD (HSD; HSD LAC; HSD LAC/CYS; HSD CYS) and viability (HSD; HSD LAC; HSD LAC/CYS; HSD CYS) and (f) lactate (HSD; HSD LAC; HSD LAC/CYS; HSD CYS) and 2-hydroxybutyrate (HSD; HSD LAC; HSD LAC/CYS) over process time. (g) Specific productivity of HSD, HSD, and HSD LAC/CYS cultivations during the entire process with mean and range. (h) Product titer over culture duration of the HSD cultivations compared to the STD fed-batch. All experiments with cell line A were conducted in duplicates ($n = 2$). Experiments with cell line B were conducted with variable replicates STD ($n = 2$), HSD ($n = 6$), HSD LAC ($n = 3$), HSD LAC/CYS ($n = 2$), and HSD CYS ($n = 1$). CYS, cysteine; HSD, high seeding densities; LAC, lactate; STD, standard; VCD, viable cell density [Color figure can be viewed at wileyonlinelibrary.com]

growth as well as specific productivities were strongly improved in the HSD LAC/CYS cultures when compared to the HSD process.

The additional supplementation of the HSD cultures with lactate and lactate/cysteine finally led to improved viable cell density profiles, cell-specific productivities, and product titers. The increase in product concentration was up to 30% in comparison to the HSD control and up to 50% in comparison to the STD fed-batch process (Figure 8a–d). Cell viabilities seemed to be positively affected by the reduced ROS formation under lactate supplemented conditions and further improved with additional cysteine. Cysteine supplementation has been shown before to affect intracellular glutathione levels, thereby actively reducing ROS (Ali et al., 2018). Interestingly, in both lactate supplemented conditions, the metabolite 2-hydroxybutyrate (2-HB) did show strongly increased concentrations in comparison to the HSD control culture (Figure 8b). Intracellular 2-HB is a side product of the cysteine synthesis from methionine (Figure 7) and is catalyzed by lactate dehydrogenase (LDH), the same enzyme that catalyzes the reaction between pyruvate and lactate (Gall et al., 2010). 2-HB accumulation was recently described to affect histone hypermethylation and further activate antioxidant pathways (Liu et al., 2018). Moreover, chemically close analogons such as 3-hydroxybutyrate (3-HB) and sodium butyrate (NaB) are known to inhibit histone deacetylation and can lead to cell cycle arrest in the G1-phase, thereby reducing cell growth and increasing cell-specific productivities (Kumar et al., 2007; Liu et al., 2018). This further matches the findings of Mulukutla et al. (2017) who reported a growth inhibitory effect of 2-HB. Furthermore, 3-HB supplementation has been reported before to increase product titers in CHO cell cultures (Chompoonuth, 2017). Thus, 2-HB accumulation might have enhanced antioxidant pathway activities, inhibited cell growth, and at the same time increased cell-specific productivities.

3.3 | Verification of optimized HSD cultivations with cell line B

To be able to derive a more comprehensive conclusion, the results were verified with a second cell line (Figure 8e–h). The same experimental conditions as before were applied for the HSD, HSD LAC, and HSD LAC/CYS cultivations with cell line B. Additionally, a single experimental condition using only cysteine bolus supplementation (HSD CYS) was evaluated to further differentiate between effects deriving from lactate or cysteine under HSD LAC/CYS conditions. Interestingly and in contrast to cell line A, supplementation of the cultivations using only lactate bolus feeding did not improve cell viabilities and viable cell densities with cell line B (Figure 8e). However, due to a slightly improved cell-specific productivity, the final product titer was increased by approx. 10% compared to the HSD control conditions (Figure 8g,h). Cysteine bolus supplementation of the HSD cultivations did lead to an improved cell viability and viable cell density profile (Figure 8e). However, since cell-specific productivities were reduced in comparison to the HSD control process, the final product concentration was only slightly improved by an increase of approx. 8% (Figure 8g,h). The combination of lactate and cysteine supplementation did show similar improvements in cell viability and viable cell density as under sole cysteine supplemented conditions (Figure 8e). Consistently to the results obtained with cell line A, the HSD LAC/CYS cultures displayed a strongly increased 2-HB concentration as well as specific productivity when compared to the HSD control culture (Figure 8f,g). The increase in cell viability, as well as specific productivity, finally led to a strong improvement in the product titer with an increase up to 47% compared to the HSD control and up to 97% when compared to the STD fed-batch process (Figure 8h).

4 | CONCLUDING REMARKS

Process intensification via N-1 perfusion and subsequent HSD cultivations can significantly increase space–time yields compared to regular fed-batch process formats. HSD cultivations have been described in literature before but limited data are available about the metabolic state of cells under HSD conditions. In this study an extended metabolite analysis in combination with FBA was used to characterize HSD cultivations in comparison to regular fed-batch processes. The analysis of potential inhibiting metabolites revealed an early accumulation of these substances in HSD cultures. Future work might address the reduction of these metabolites by media adaptions targeting their metabolic precursors, similar to the work from Muluktula et al. (2017). However, the primary goal in this study was to increase the cells longevity and specific productivity rather than to further increase peak cell densities. The FBA did reveal distinct metabolic phases with high formation of ROS and high cell-specific productivities in the HSD cultures. Based on these results the feeding strategy was adapted and supplementation of the cultures with lactate and cysteine did improve the process performance. The strong combinational effect of lactate and cysteine supplementation, demonstrated with cell lines A and B, indicates that these two media components exert synergistic effects on the cell's metabolism. Whereas the additional supplementation of the cultures with lactate did reduce the intracellular ROS formation, further supplementation of cysteine probably led to active reduction of intracellular ROS via the glutathione pathway. Thus, both media components contributed to an improved intracellular ROS balance. Interestingly, lactate supplemented cultures did show an increased cell-specific productivity. The metabolite 2-HB was strongly elevated in these cultures, indicating that it might be correlated to the improved productivity similar to its chemical analogons such as 3-HB and NaB. Further reduction of ROS species via media optimization of antioxidant compounds such as vitamins, thiols, or α-ketoacids as well as genetic engineering approaches could further improve culture longevity in HSD processes (Chevallier et al., 2020; Henry et al., 2020). At the same time strategies to induce cell cycle arrest and thereby increase specific productivities via temperature shifts or media components such as sodium butyrate, pentanoic acid, or resveratrol (Kumar et al., 2007; McHugh et al., 2020; Toronjo-Urquiza et al., 2019) could enhance the productivity of HSD cultures.

Finally, the application of metabolic modeling approaches in this study led to optimized HSD cultivations with a titer increase up to 47%. Based on the gathered data and metabolic analysis further targeted optimization strategies can be applied in the future since the full potential of HSD cultivations is still to be reached.

CONFLICT OF INTERESTS

The authors declare that there are no conflict of interests.

AUTHOR CONTRIBUTIONS

Matthias Brunner: *Conceptualization, experimental design, methodology, data analysis, visualization and writing*. Klara Kolb: *Data analysis, visualization and review*. Alena Keitel: *Coordination of experiments, experimental design and review*. Fabian Stiefel: *Experimental design and review*. Thomas Wucherpfennig: *Supervision and review*. Jan Bechman: *Experimental design, supervision, and review*. Andreas Unsöld: *Supervision and review*. Jochen Schaub: *Supervision, resources, and review*.

ORCID

Matthias Brunner http://orcid.org/0000-0003-3816-9365

REFERENCES

Ahn, W. S., & Antoniewicz, M. R. (2011). Metabolic flux analysis of CHO cells at growth and non-growth phases using isotopic tracers and mass spectrometry. *Metabolic Engineering*, *13*(5), 598–609. https://doi.org/10.1016/j.ymben.2011.07.002

Ali, A. S., Raju, R., Kshirsagar, R., Ivanov, A. R., Gilbert, A., Zang, L., & Karger, B. L. (2018). Multi-omics study on the impact of cysteine feed level on cell viability and mAb production in a CHO bioprocess. *Biotechnology Journal*, *14*(4), 1800352. https://doi.org/10.1002/biot.201800352

Becker, M., Junghans, L., Teleki, A., Bechmann, J., & Takors, R. (2019). Perfusion cultures require optimum respiratory ATP supply to maximize cell specific and volumetric productivities. *Biotechnology and Bioengineering*, *116*(5), 951–960. https://doi.org/10.1002/bit.26926

Bielser, J. M., Wolf, M., Souquet, J., Broly, H., & Morbidelli, M. (2018). Perfusion mammalian cell culture for recombinant protein manufacturing - A critical review. *Biotechnology Advances*, *36*(4), 1328–1340. https://doi.org/10.1016/j.biotechadv.2018.04.011

Chevallier, V., Andersen, M. R., & Malphettes, L. (2020). Oxidative stress-alleviating strategies to improve recombinant protein production in CHO cells. *Biotechnology and Bioengineering*, *117*(4), 1172–1186. https://doi.org/10.1002/bit.27247

Chompoonuth, P. (2017). *Metabolite profiling associated with productive recombinant CHO cell culture*. (PhD thesis). The University of Manchester. Retrieved from https://www.research.manchester.ac.uk/portal/en/theses/metabolite-profiling-associated-with-productive-recombinant-cho-cell-culture(3bb6bdaf-d8dc-4249-b77b-159e9e77307a).html

Chong, W. P. K., Yusufi, F. N. K., Lee, D.-Y., Reddy, S. G., Wong, N. S. C., Heng, C. K., Yap, M. G. S., & Ho, Y. S. (2011). Metabolomics-based identification of apoptosis-inducing metabolites in recombinant fed-batch CHO culture media. *Journal of Biotechnology*, *151*(2), 218–224. https://doi.org/10.1016/j.jbiotec.2010.12.010

Duarte, T. M., Carinhas, N., Barreiro, L. C., Carrondo, M. J. T., Alves, P. M., & Teixeira, A. P. (2014). Metabolic responses of CHO cells to limitation of key amino acids. *Biotechnology and Bioengineering*, *111*(10), 2095–2106. https://doi.org/10.1002/bit.25266

Forkink, M., Smeitink, J. A. M., Brock, R., Willems, P. H. G. M., & Koopman, W. J. H. (2010). Detection and manipulation of mitochondrial reactive oxygen species in mammalian cells. *Biochimica et Biophysica Acta—Bioenergetics*, *1797*(6), 1034–1044. https://doi.org/10.1016/j.bbabio.2010.01.022

Gall, W. E., Beebe, K., Lawton, K. A., Adam, K.-P., Mitchell, M. W., Nakhle, P. J., Ryals, J. A., Milburn, M. V., Nannipieri, M., Camastra, S., Natali, A., & Ferrannini, E. (2010). Alpha-hydroxybutyrate is an early biomarker of insulin resistance and glucose intolerance in a nondiabetic population. *PLOS One*, *5*(5), e10883. https://doi.org/10.1371/journal.pone.0010883

Ghaffari, N., Jardon, M. A., Krahn, N., Butler, M., Kennard, M., Turner, R. F. B., & Piret, J. M. (2019). Effects of cysteine, asparagine or glutamine limitations in CHO cell batch and fed-batch cultures. *Biotechnology Progress*, *36*(2), e2946. https://doi.org/10.1002/btpr.2946

Goudar, C., Biener, R., Boisart, C., Heidemann, R., Piret, J., de Graaf, A., & Konstantinov, K. (2010). Metabolic flux analysis of CHO cells in perfusion culture by metabolite balancing and 2D [13C, 1H] COSY NMR spectroscopy. *Metabolic Engineering*, *12*(2), 138–149. https://doi.org/10.1016/j.ymben.2009.10.007

Hansen, H. A., & Emborg, C. (1994). Influence of ammonium on growth, metabolism, and productivity of a continuous suspension Chinese hamster ovary cell culture. *Biotechnology Progress*, *10*(1), 121–124. https://doi.org/10.1021/bp00025a014

Henry, M. N., MacDonald, M. A., Orellana, C. A., Gray, P. P., Gillard, M., Baker, K., & Martínez, V. S. (2020). Attenuating apoptosis in Chinese hamster ovary cells for improved biopharmaceutical production. *Biotechnology and Bioengineering*, *117*(4), 1187–1203. https://doi.org/10.1002/bit.27269

Ivarsson, M., Noh, H., Morbidelli, M., & Soos, M. (2015). Insights into pH-induced metabolic switch by flux balance analysis. *Biotechnology Progress*, *31*(2), 347–357. https://doi.org/10.1002/btpr.2043

Karst, D. J., Steinebach, F., Soos, M., & Morbidelli, M. (2017). Process performance and product quality in an integrated continuous antibody production process. *Biotechnology and Bioengineering*, *114*(2), 298–307. https://doi.org/10.1002/bit.26069

Krattenmacher, F., Heermann, T., Calvet, A., Krawczyk, B., & Noll, T. (2018). Effect of manufacturing temperature and storage duration on stability of chemically defined media measured with LC-MS/MS. *Journal of Chemical Technology & Biotechnology*, *94*(4), 1144–1155. https://doi.org/10.1002/jctb.5861

Kumar, N., Gammell, P., & Clynes, M. (2007). Proliferation control strategies to improve productivity and survival during CHO based production culture: A summary of recent methods employed and the effects of proliferation control in product secreting CHO cell lines. *Cytotechnology*, *53*(1–3), 33–46. https://doi.org/10.1007/s10616-007-9047-6

Lao, M.-S., & Toth, D. (1997). Effects of ammonium and lactate on growth and metabolism of a recombinant Chinese hamster ovary cell culture. *Biotechnology Progress*, *13*(5), 688–691. https://doi.org/10.1021/bp9602360

Lindskog, E. K. (2018). Chapter 5—Upstream bioprocessing: Basic concepts. In (Eds.) Jagschies, G., Lindskog, E., Łącki, K. & Galliher, P., *Biopharmaceutical processing* (pp. 97–110). Elsevier.

Liu, Y., Guo, J.-Z., Liu, Y., Wang, K., Ding, W., Wang, H., Liu, X., Zhou, S., Lu, X. C., Yang, H. B., Xu, C., Gao, W., Zhou, L., Wang, Y. P., Hu, W., Wei, Y., Huang, C., & Lei, Q. Y. (2018). Nuclear lactate dehydrogenase A senses ROS to produce α-hydroxybutyrate for HPV-induced cervical tumor growth. *Nature Communications*, *9*(1), 4429. https://doi.org/10.1038/s41467-018-06841-7

McHugh, K. P., Xu, J., Aron, K. L., Borys, M. C., & Li, Z. J. (2020). Effective temperature shift strategy development and scale confirmation for simultaneous optimization of protein productivity and quality in Chinese hamster ovary cells. *Biotechnology Progress*, *36*(3):e2959. https://doi.org/10.1002/btpr.2959

Mulukutla, B. C., Gramer, M., & Hu, W.-S. (2012). On metabolic shift to lactate consumption in fed-batch culture of mammalian cells.

Metabolic Engineering, *14*(2), 138–149. https://doi.org/10.1016/j.ymben.2011.12.006

Mulukutla, B. C., Kale, J., Kalomeris, T., Jacobs, M., & Hiller, G. W. (2017). Identification and control of novel growth inhibitors in fed-batch cultures of Chinese hamster ovary cells. *Biotechnology and Bioengineering*, *114*, 1779–1790. https://doi.org/10.1002/bit.26313

Padawer, I., Ling, W. L. W., & Bai, Y. (2013). Case Study: An accelerated 8-day monoclonal antibody production process based on high seeding densities. *Biotechnology Progress*, *29*(3), 829–832. https://doi.org/10.1002/btpr.1719

Pereira, S., Kildegaard, H. F., & Andersen, M. R. (2018). Impact of CHO metabolism on cell growth and protein production: An overview of toxic and inhibiting metabolites and nutrients. *Biotechnology Journal*, *13*(3), 1700499. https://doi.org/10.1002/biot.201700499

Pohlscheidt, M., Jacobs, M., Wolf, S., Thiele, J., Jockwer, A., Gabelsberger, J., Jenzsch, M., Tebbe, H., & Burg, J. (2013). Optimizing capacity utilization by large scale 3000 L perfusion in seed train bioreactors. *Biotechnology Progress*, *29*(1), 222–229. https://doi.org/10.1002/btpr.1672

Popp O., Müller, D., Didzus, K., Paul, W., Lipsmeier, F., Kirchner, F., Niklas, J., Mauch, K., & Beaucamp, N. (2016). A hybrid approach identifies metabolic signatures of high-producers for Chinese hamster ovary clone selection and process optimization. *Biotechnology and Bioengineering*, *113*(9), 2005–2019. https://doi.org/10.1002/bit.25958

Prade, E., Zeck, A., Stiefel, F., Unsoeld, A., Mentrup, D., Arango Gutierrez, E., & Gorr, I. H. (2020). Cysteine in cell culture media induces acidic IgG1 species by disrupting the disulfide bond network. *Biotechnology and Bioengineering*, 1–14. https://doi.org/10.1002/bit.27628

Ritacco, F. V., Wu, Y., & Khetan, A. (2018). Cell culture media for recombinant protein expression in Chinese hamster ovary (CHO) cells: History, key components, and optimization strategies. *Biotechnology Progress*, *34*, 1407–1426. https://doi.org/10.1002/btpr.2706

Schaub, J., Clemens, C., Kaufmann, H., & Schulz, T. W. (2012). Advancing biopharmaceutical process development by system-level data analysis and integration of omics data. *Advances in Biochemical Engineering/Biotechnology*, *127*, 133–163. https://doi.org/10.1007/10_2010_98

Sengupta, N., Rose, S. T., & Morgan, J. A. (2011). Metabolic flux analysis of CHO cell metabolism in the late non-growth phase. *Biotechnology and Bioengineering*, *108*(1), 82–92. https://doi.org/10.1002/bit.22890

Stepper, L., Filser, F. A., Fischer, S., Schaub, J., Gorr, I., & Voges, R. (2020). Pre-stage perfusion and ultra-high seeding cell density in CHO fed-batch culture: A case study for process intensification guided by systems biotechnology. *Bioprocess and Biosystems Engineering*, *43*, 1431–1443. https://doi.org/10.1007/s00449-020-02337-1

Toronjo-Urquiza, L., Acosta-Martin, A. E., James, D. C., Nagy, T., & Falconer, R. J. (2019). Resveratrol addition to CHO cell culture media: The effect on cell growth, monoclonal antibody synthesis and its chemical modification. *Biotechnology Progress*, *36*(3):e2940. https://doi.org/10.1002/btpr.2940

Wahrheit, J., Niklas, J., & Heinzle, E. (2014). Metabolic control at the cytosol–mitochondria interface in different growth phases of CHO cells. *Metabolic Engineering*, *23*, 9–21. https://doi.org/10.1016/j.ymben.2014.02.001

Walsh, G. (2018). Biopharmaceutical benchmarks 2018. *Nature Biotechnology*, *36*(12), 1136–1145. https://doi.org/10.1038/nbt.4305

Walther, J., Lu, J., Hollenbach, M., Yu, M., Hwang, C., McLarty, J., & Brower, K. (2019). Perfusion cell culture decreases process and product heterogeneity in a head-to-head comparison with fed-batch. *Biotechnology Journal*, *14*(2), 1700733. https://doi.org/10.1002/biot.201700733

Wang, J., Zhou, L., Lei, H., Hao, F., Liu, X., Wang, Y., & Tang, H. (2017). Simultaneous quantification of amino metabolites in multiple metabolic pathways using ultra-high performance liquid chromatography with tandem-mass spectrometry. *Scientific Reports*, *7*(1), 1423. https://doi.org/10.1038/s41598-017-01435-7

Xu, S., Gavin, J., Jiang, R., & Chen, H. (2017). Bioreactor productivity and media cost comparison for different intensified cell culture processes. *Biotechnology Progress*, *33*(4), 867–878. https://doi.org/10.1002/btpr.2415

Yang, W. C., Lu, J., Kwiatkowski, C., Yuan, H., Kshirsagar, R., Ryll, T., & Huang, Y.-M. (2014). Perfusion seed cultures improve biopharmaceutical fed-batch production capacity and product quality. *Biotechnology Progress*, *30*(3), 616–625. https://doi.org/10.1002/btpr.1884

Zhao, R.-Z., Jiang, S., Zhang, L., & Yu, Z.-B. (2019). Mitochondrial electron transport chain, ROS generation and uncoupling. *International Journal of Molecular Medicine*, *44*(1), 3–15. https://doi.org/10.3892/ijmm.2019.4188

SUPPORTING INFORMATION

Additional Supporting Information may be found online in the supporting information tab for this article.

How to cite this article: Brunner M, Kolb K, Keitel A, et al. Application of metabolic modeling for targeted optimization of high seeding density processes. *Biotechnology and Bioengineering*. 2021;118:1793–1804. https://doi.org/10.1002/bit.27693